Coherent imaging using cross-correlations of ambient noise sources

A. Semin[†,*], **C. Tsogka**[†,*]
[†]Institute of Applied and Computational Mathematics, FORTH, Heraklion
[*]Email: asemin@iacm.forth.gr, tsogka@iacm.forth.gr

Talk Abstract

We consider here the problem of imaging using passive incoherent recordings due to ambient noise sources. The first step towards imaging in this configuration is the computation of the cross-correlations of the recorded signals. These cross-correlations are computed between pairs of sensors (receivers) and contain very important information about the background medium. They can be used, for example, to compute the travel time between sensors or even the Green's function from one sensor to the other. Our aim is to use these cross-correlations in order to image reflectors embedded in clutter. To do so we will use coherent imaging methods, such as travel time migration and coherent interferometry (CINT) [9], [10].

1 Introduction

It is well known [1], [2], [3], [4] that cross-correlations of signals recorded at passive sensors generated by ambient noise sources can be used for the estimation of the Green's function in-between the sensors. Although the theory states that the full Green's function can be obtained [5], [6], in practice for imaging applications [1], [2], or for background velocity estimation [7], extracting the travel time between the two sensors is enough.

Here the sensors are called passive because we assume that they can only play the role of receivers. The estimation of the travel time between the passive sensors is possible when the ambient noise sources are randomly distributed, uncorrelated and extend overall the whole space, while they are statistically stationary in time [6]. These assumptions, however, are not always satisfied in applications where the noise source distribution is usually spatially limited [8]. In that case, and for a homogeneous background medium, it was shown in [1] that the estimation of the travel time between the two sensors is possible when the ray that connects the two sensors goes through the source region. When the background medium, however, contains random inhomogeneities that cause multiple scattering, the directional diversity of the noisy signals is enhanced and estimation of the travel time is possible for sensor configurations that do not fulfill the above mentioned geometric condition (cf. [2]).

Our starting point is the analysis of J. Garnier and G. Papanicolaou about passive sensor imaging using cross-correlations generated by ambient noise sources [1], [2]. When there is no clutter, or the clutter is weak, migration is expected to work well, as for the active array imaging problem [9]. When the clutter is significant, migration is expected to produce heavily speckled and unreliable images. In that case, we propose the use of CINT [9], [10], a statistically stable imaging method that produces images with negligible fluctuations induced by scattering in clutter. We consider in this paper the case of homogeneous and weak cluttered media. Stronger cluttered media will be considered in the future.

2 Simulation setup and mathematical model

We consider $u(\mathbf{x},t)$ the solution of the acoustic wave equation

$$\frac{1}{c^2(\mathbf{x})}\frac{\partial^2 u(\mathbf{x},t)}{\partial t^2} - \Delta u(\mathbf{x},t) = n(\mathbf{x},t), \qquad (1)$$

in two dimensions, $\mathbf{x} = (x,z)$, in a medium with propagation speed $c(\mathbf{x})$ given by

$$\frac{1}{c^2(\mathbf{x})} = \frac{1}{c_0^2(\mathbf{x})}\left[1 + \sigma\mu\left(\frac{x}{\ell_x},\frac{z}{\ell_z}\right)\right]. \qquad (2)$$

Here $c_0(\mathbf{x})$ is the smooth and known speed of sound in the background medium. The normalized fluctuations are modeled by $\mu(\mathbf{x})$, which is a statistically homogeneous random process with mean zero and rapidly decaying correlation. The fluctuations vary on the characteristic length scales (ℓ_x,ℓ_z), the correlation lengths in the (x,z) directions, which can be considered to be the typical size of the inhomogeneities. The parameter σ controls the strength of the fluctuations.

We solve the acoustic wave equation with the software Montjoie (*https://gforge.inria.fr/projects/montjoie*) using mixed spectral finite elements [11] of 4th order in space and a finite difference discretization of 4th order in time. We simulate wave propagation in an unbounded environment by surrounding the computational domain with a perfectly matched absorbing layer (PML).

In (1), $n(\mathbf{x},t)$ models the noise sources. It is a zero mean stationary (in time) random process with correlation function,

$$E\{n(\mathbf{x}_1,t_1)n(\mathbf{x}_2,t_2)\} = \mathbb{F}(t_1-t_2)K(\mathbf{x}_1)\delta(\mathbf{x}_1-\mathbf{x}_2).$$

The process n is delta-correlated in space and K characterizes the spatial support of the sources. The time distribution of the noise sources is characterized by the correlation function $\mathbb{F}(t_2 - t_1)$, which in our numerical simulations is given by

$$\mathbb{F}(t) = \int F(\tau)F(t+\tau)d\tau, \tag{3}$$

$$F(t) = \mathrm{sinc}(Bt)\cos(2\pi f_0 t)\exp(-t^2/(2C_t^2)). \tag{4}$$

Here C_t is the correlation length in time, B the bandwidth, and f_0 the central frequency of the sources.

3 Discrete wave cross-correlation

Let $(u(\mathbf{x}_1)_n)_{0\le n<N}$ and $(u(\mathbf{x}_2)_n)_{0\le n<N}$ denote the time-dependant wave fields recorded by two sensors at $\mathbf{x}_1$ and $\mathbf{x}_2$ and at discrete time $t_n = n\delta_t$, for $0 \le n < N$. Their cross-correlation function over the time interval $[-T, T]$, with $T = N\delta_t$, and with time lag $\tau = \nu\delta_t$ is given by

$$C_T(\tau, \mathbf{x}_1, \mathbf{x}_2) = \frac{1}{N}\sum_{n=0}^{N-1-\nu} u(\mathbf{x}_1)_n u(\mathbf{x}_2)_{n+\nu}. \tag{5}$$

Implementing directly (5) in a numerical code is quite easy, but execution time is in $O(N^2)$. Since this formula is close to a discrete convolution formula, we wish to use the Discrete Fourier Transform (DFT) as defined in the GNU Scientific Library [12]. In this case, we extend the wave fields $(u(\mathbf{x})_n)_{0\le n<N}$, for $\mathbf{x} = \{\mathbf{x}_1, \mathbf{x}_2\}$, to $(\tilde{u}(\mathbf{x})_n)_{0\le n<2N}$ defined as

$$\tilde{u}(\mathbf{x})_n = \begin{cases} u_{n-N}, & n \ge N, \\ 0, & \text{otherwise}. \end{cases} \tag{6}$$

We can rewrite the cross-correlation function (5) as, (for the second index we take the remaining in $\{0, \ldots, 2N-1\}$ *modulo* $2N$),

$$C_T(\mathbf{x}_1, \mathbf{x}_2)_{N+\nu} = \frac{1}{N}\sum_{n=0}^{2N-1} \tilde{u}(\mathbf{x}_1)_n\, \tilde{u}(\mathbf{x}_2)_{n+\nu}, \tag{7}$$

for $-N \le \nu < N$.

We recall here the DFT,

$$\mathcal{F}(u)_k = \sum_{n=0}^{2N-1} u_n \exp\left(-2\imath\pi\frac{kn}{2N}\right). \tag{8}$$

Proposition 3.1. *The following relation holds,*

$$\mathcal{F}(C_T(\mathbf{x}_1, \mathbf{x}_2))_k = \frac{(-1)^k}{N}\mathcal{F}(\tilde{u}(\mathbf{x}_1))_{-k}\,\mathcal{F}(\tilde{u}(\mathbf{x}_2))_k. \tag{9}$$

Relation (9) allows us to compute $C_T(\mathbf{x}_1, \mathbf{x}_2)$ in $O(N)$ steps. Moreover, since the recorded wave fields are real valued, we can rewrite this relation as

$$\mathcal{F}(C_T(\mathbf{x}_1, \mathbf{x}_2))_k = \frac{(-1)^k}{N}\overline{\mathcal{F}(\tilde{u}(\mathbf{x}_1))_k}\mathcal{F}(\tilde{u}(\mathbf{x}_2))_k. \tag{10}$$

Computing relation (10) is also in $O(N)$, and has its own interest from a computational point of view.

4 Migration Imaging

For this section and the next one, we shall assume that the noise sources are spatially localized and the sensors $(\mathbf{x}_j)_{1\le j\le J}$ are located between the sources and the reflectors. More precisely, rays going through reflectors and sensors reach into the source region, and the sensors are between the reflectors and the sources along these rays. We call this the daylight configuration.

Stationary phase analysis done by J. Garnier and G. Papanicolaou [1] shows that the cross-correlation between two sensors $\mathbf{x}_i$ and $\mathbf{x}_j$ is expected to have two peaks: one at the travel time between the two sensors and another one at the sum of the travel times between the sensors and the scatterer. To keep only the interesting peak that concerns the scatterer, the image at a search point $\mathbf{z}$ is computed using the following daylight imaging functional (cf. [1]),

$$\mathcal{I}^{\mathrm{D}}(\mathbf{z}) = 2\sum_{j,l=1}^{J} C^{\mathrm{sym}}_{T,\mathrm{coda}}(\tau(\mathbf{z}, \mathbf{x}_l) + \tau(\mathbf{z}, \mathbf{x}_j), \mathbf{x}_j, \mathbf{x}_l), \tag{11}$$

where $\tau(\mathbf{z}, \mathbf{x}_l)$ is the travel time between $\mathbf{x}_l$ and $\mathbf{z}$:

$$\tau(\mathbf{z}, \mathbf{x}_l) = \frac{|\mathbf{z} - \mathbf{x}_l|}{c_0}, \tag{12}$$

and

$$C^{\mathrm{sym}}_{T,\mathrm{coda}}(\tau, \mathbf{x}_j, \mathbf{x}_l) = \big(C_T(\tau, \mathbf{x}_j, \mathbf{x}_l) + C_T(-\tau, \mathbf{x}_j, \mathbf{x}_l)\big)1_{[\tau(\mathbf{x}_j, \mathbf{x}_l), +\infty]}. \tag{13}$$

If we consider that the scatterer is far enough from the receivers, then we can simplify formula (11). The precise statement is the following:

Proposition 4.1. *The migration imaging functional with daylight illumination is given by*

$$\mathcal{I}^{\mathrm{D}}(\mathbf{z}) = 2\sum_{j,l=1}^{J} C_T(\tau(\mathbf{z}, \mathbf{x}_l) + \tau(\mathbf{z}, \mathbf{x}_j), \mathbf{x}_j, \mathbf{x}_l) \tag{14}$$

5 Numerical simulations

We study the acoustic wave propagation on the rectangle $[0, 50\lambda] \times [-15\lambda, 15\lambda]$, with a reflector located in $[44\lambda, 46\lambda] \times [-\lambda, \lambda]$. The random distribution of sources has support on the rectangle $[0, 4\lambda] \times [-15\lambda, 15\lambda]$ (gray region on Figure 1), and we record the solution u of the wave equation at $J = 61$ sensors located at $\mathbf{x}_j = (5\lambda, (j-31)\lambda/2)$, for $1 \le j \le 61$. Length is scaled by the reference wavelength $\lambda = 500$m. The reflector is modeled as a soft acoustic scatterer, *i.e.*, $u = 0$ on the boundary of the reflector.

Figure 1: Geometry of the passive sensor imaging problem for a daylight illumination.

In our simulations we consider for simplicity that the wave speed in (2) fluctuates about a constant value $c_0(\mathbf{x}) = 1.5$Km/s. We shall show results for two cases, a homogeneous background medium ($\mu = 0$), and a layered random medium, for which the fluctuation process μ varies only in the x direction ($\mu = \mu(x)$) and its correlation function is

$$E\{\mu(x_1)\mu(x_2)\} = \left(1 + \frac{|x_1 - x_2|}{\ell_x}\right) e^{-\frac{|x_1-x_2|}{\ell_x}}.$$

In the numerics we used $\ell_x = 25$m and $\sigma = 0.02$. The corresponding velocity profile is shown on Figure 2.

To model the noise sources we use (4) with $f_0 = 3$Hz, $C_t = 0.25$s and $B = 3$Hz.

Using the daylight imaging functional (14) we compute the image near the scatterer. We show the results for the homogeneous background medium on figure 3 and for the layered medium on Figure 4. In both cases observe that we can recover the location of the scatterer. Moreover, the signal to noise ratio of the image is very good, *i.e.*, we only have one maximum at the correct scatterer location and the noise level is low. The question that naturally arises is "Under what conditions do we obtain such a good image?" or in other words "What are the parameters that control the quality of the image, and how?" A partial answer to this question is that the signal to noise ratio (SNR)

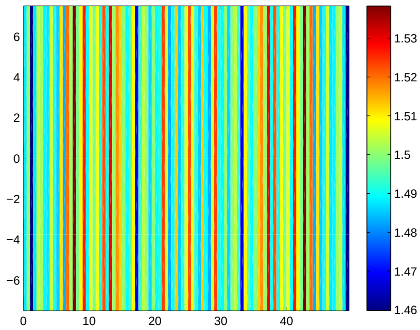

Figure 2: Wave speed $c(\mathbf{x})$ in the random layered medium. Length is measured in wavelengths λ and the wave speed in Km/s.

of the image increases with the number of the receivers, the number of the sources, and the recording time. We are currently working on a theoretical and numerical study of the SNR of the image.

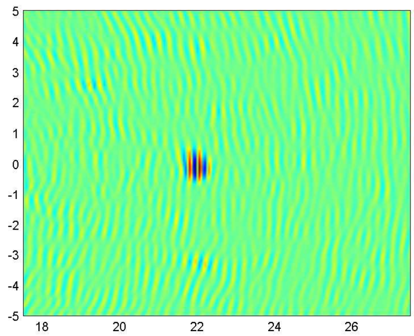

Figure 3: Daylight imaging functional (14) for the homogeneous background medium. Length is in Km.

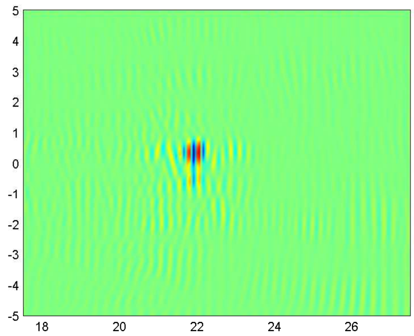

Figure 4: Daylight imaging functional (14) for the layered medium shown on Figure 2. Length is in Km.

Acknowledgments

This work was partially supported by the European Research Council Starting Grant, GA 239959 and the FP7-REGPOT-2009-1 project “Archimedes Center for Modeling, Analysis and Computation”.

References

[1] J. Garnier and G. Papanicolaou, “Passive sensor imaging using cross correlations of noisy signals in a scattering medium”, SIAM J. Imaging Sciences, Vol. 2, pp. 396–437, 2009.

[2] J. Garnier and G. Papanicolaou, “Resolution enhancement from scattering in passive sensor Imaging with Cross Correlations”, preprint, 2010.

[3] Y. Colin de Verdière, “Semiclassical analysis and passive imaging”, Nonlinearity, Vol. 22, pp. R45–R75, 2009.

[4] K. Wapenaar and J. Fokkema, “Green’s function representations for seismic interferometry”, Geophysics, Vol. 71, pp. SI33–SI46, 2006.

[5] R. Snieder, “Extracting the Green’s function from the correlation of coda waves: A derivation based on stationary phase”, Phys. Rev. E, Vol. 69, 046610, 2004.

[6] P. Roux, K. G. Sabra, W. A. Kuperman, and A. Roux, “Ambient noise cross correlation in free space: Theoretical approach”, J. Acoust. Soc. Am., Vol. 117, pp. 79–84, 2005.

[7] K. G. Sabra, P. Gerstoft, P. Roux, and W. Kuperman, “Surface wave tomography from microseisms in Southern California”, Geophys. Res. Lett., Vol. 32, L14311, 2005.

[8] L. Stehly, M. Campillo, and N. M. Shapiro, “A study of the seismic noise from its long-range correlation properties”, Geophys. Res. Lett., Vol. 111, B10306, 2006.

[9] L. Borcea, G. Papanicolaou and C. Tsogka, “Interferometric array imaging in clutter”, Inverse Problems, vol 21, pp. 1419-1460, 2005.

[10] L. Borcea, G. Papanicolaou and C. Tsogka, “Adaptive interferometric imaging in clutter and optimal illumination”, Inverse Problems, vol. 22, pp. 1405-1436, 2006.

[11] G. Cohen, “Higher-order numerical methods for transient wave equations”, Springer-Verlag, 2002.

[12] M. Galassi, J. Davies, J. Theiler, B. Gough, G. Jungman, M. Booth and F. Rossi, “GNU Scientific Library Reference Manual”, Revised Second Edition (v1.8), Network Theory Ltd, 2006.